The Journal of Chemical Physics

RESEARCH ARTICLE | JUNE 22 2026

Partial oxidation of methane to methanol is made possible with metal monoxide anions

Tatsuya Chiba ; Benjamin R. Bilik ; Kathryn Foreman ; Shiying Wang ; Yuheng Han ; Eslam F. M. Abdelazim ; Safaa Sader ; Evangelos Miliordos ; Kit H. Bowen

J. Chem. Phys. 164, 244303 (2026)
https://doi.org/10.1063/5.0332490

The Journal of Chemical Physics ARTICLE pubs.aip.org/aip/jcp

Partial oxidation of methane to methanol is made possible with metal monoxide anions

Cite as: J. Chem. Phys. 164, 244303 (2026); doi: 10.1063/5.0332490
Submitted: 4 March 2026 • Accepted: 5 June 2026 •
Published Online: 22 June 2026

Tatsuya Chiba,[1] Benjamin R. Bilik,[1] Kathryn Foreman,[1] Shiying Wang,[1] Yuheng Han,[1] Eslam F. M. Abdelazim,[2] Safaa Sader,[2,a)] Evangelos Miliordos,[2,b)] and Kit H. Bowen[1,b)]

AFFILIATIONS

[1] Department of Chemistry, Johns Hopkins University, Baltimore, Maryland 21218, USA
[2] Department of Chemistry and Biochemistry, Auburn University, Auburn, Alabama 36849, USA

[a)] **Present address:** Department of Chemistry and Biochemistry, University of Notre Dame, Notre Dame, Indiana 46556, USA.
[b)] **Authors to whom correspondence should be addressed:** emiliord@auburn.edu and kbowen@jhu.edu

ABSTRACT

Previous calculations have shown that certain transition metal monoxide anions have an advantage in catalyzing the partial oxidation of CH_4 to CH_3OH, viz., $MO^- + CH_4 \rightarrow M^- + CH_3OH$, because their anionic metal centers interact only weakly with the methanol product, thus preventing its over-oxidation to formaldehyde. In this study, the oxidation of methane to methanol by NiO^- was demonstrated experimentally by cryo-trapping the neutral reaction products onto a substrate and then characterizing the eluded product via temperature-programmed desorption. This work both vindicates the previous calculations and presents a proof-of-principle example. Concurrent calculations showed this reaction to selectively form methanol to the detriment of other products.

I. INTRODUCTION

The utilization of abundant methane reserves has been a topic of intense research over the past three decades.[1,2] The large quantities of natural gas (mostly methane) extracted from oil wells and fracking sites could be used not only as fuel but also, in an environmentally friendlier way, as feedstock for making a variety of high value chemicals.[1] Ideally, methane would be functionalized at its extraction site under mild conditions. The conversion of methane to methanol is especially beneficial, since methanol is a liquid (facilitating transportation), it exhibits a high heat of combustion (providing quality fuel), it is among the most widely used solvents in industry, and it is readily converted to other chemicals. Nevertheless, despite efforts and progress made at the laboratory level,[3] the idea of a "methanol economy" has not yet been realized.[4]

The main bottleneck is that a low-cost process for the partial oxidation of methane to methanol with a simultaneously large conversion rate and high selectivity is not known.[5] While the Periana catalyst achieves both high rates and selectivity,[6] the oxidants it uses and the necessity of recycling its protecting chemical groups have impeded its implementation.[7] The fundamental reason for the difficulty in selectively oxidizing methane is that the C–H bond in methane is stronger than it is in methanol. Thus, a catalyst, capable of activating methane, can also activate methanol.[5,7] Recent quantum chemical calculations identify two possible types of molecular metal-oxide catalysts with the capability of bypassing this "dead-end" route.[8] Hydrophilic ligands making hydrogen bonds with methanol can specifically distort the transition state, increasing its activation barrier to values comparable with or larger than that with methane.[9] The other type pertains to negatively charged metal monoxide catalysts. At the methanol formation step in the catalytic cycle (see structures in green in Fig. 1), the metal atomic anion, M^-, interacts only weakly with the nascently produced methanol (as opposed to the strong interaction of metal cations with methanol), allowing for its faster removal from the catalyst.[10,11] This kinetically based strategy had been broadly proposed in the literature[7] and it has been applied in electrochemistry experiments.[12] It should be stressed that anionic metal oxides with more than one metal-oxygen bonds, and which have been studied previously,[13] do not result in the same favorable outcome. The reason is that the metal center does not necessarily adopt a −1 charge after the formation of methanol.

This work presents the first experimental evidence for the partial oxidation of methane to methanol using an anionic metal monoxide, specifically NiO^-. Mass spectra (cationic) of the neutral reaction products, generated in the gas-phase, ion-neutral reaction, $NiO^- + CH_4 \rightarrow Ni^- + CH_3OH$, confirm earlier theoretical

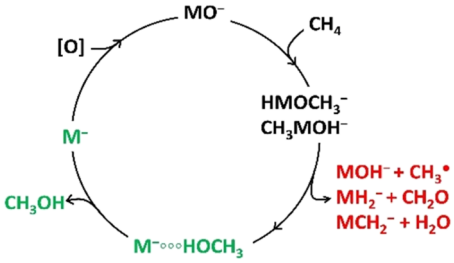

FIG. 1. Typical catalytic cycle for the oxidation of methane facilitated by a metal oxide anion (MO^-). The desired/unwanted products are represented in green/red, respectively, with [O] representing an oxidant.

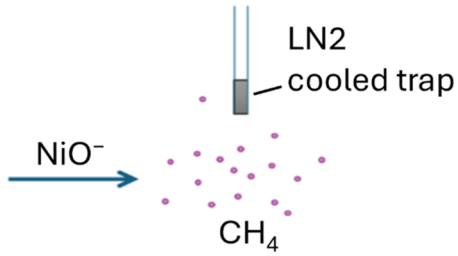

FIG. 2. Schematic description of the essential aspects of the experiment. A mass-selected beam of NiO^- interacted with a low-density cloud of CH_4. The condensable neutral reaction products were collected by using a liquid-nitrogen-cooled cryo-trap.

results.[10,11] It is also shown in the following that NiO^- avoids the formation of byproducts, such as $CH_3^{\cdot}$ and CH_2O, and the $NiCH_2^-$ poisoning intermediate.

II. METHODS

Essential aspects of the experiment are shown schematically in Fig. 2; there, a mass-selected beam of NiO^- interacts with a low-density cloud of CH_4, where the reaction takes place. This is a beam–gas experiment. A nearby liquid-nitrogen-cooled cryo-trap then captures the condensable neutral reaction products, which are subsequently thermally eluded and examined mass spectrometrically. The apparatus used in these experiments is shown schematically in Fig. 3. This instrument, which we normally use for beam deposition/surface characterization experiments,[14] was re-purposed for these experiments. It has all of the attributes needed for this work, i.e., an anion source for making NiO^-, a quadrupole mass spectrometer for mass-selecting the NiO^- anions, an ultra-high vacuum chamber, where gas density can be controlled and NiO^-/CH_4 collisions can occur, a cold-finger for collecting reaction products, and a residual gas analyzer, RGA (consisting of an electron bombardment ionizer, another quadrupole mass spectrometer, and an electron multiplier cation detector) for detecting and mass-characterizing the neutral reaction products via the classic temperature programmed desorption (TPD) technique.

Specifically, NiO^- anions were produced by ablating a rotating and translating nickel rod with a diameter of 0.25 in. with the second harmonic (532 nm) output of a Nd:YAG laser (Innolas, SpitLight, DPSS 250) at 150 Hz, while almost simultaneously pulsing a 10% N_2O in He gas mixture (80 psig) over the rod. The resultant anions were transported by both quadrupolar and octopolar ion guides through a 90° quadrupole ion bender (which separated them from any cations) before being directed through a quadrupole mass filter (Extrel, QPS4000, 150QC, 440 kHz, 19 mm diameter rods) for mass analysis and mass selection. The mass-selected NiO^- beam (~300 pA) was then directed into an ultra-high-vacuum

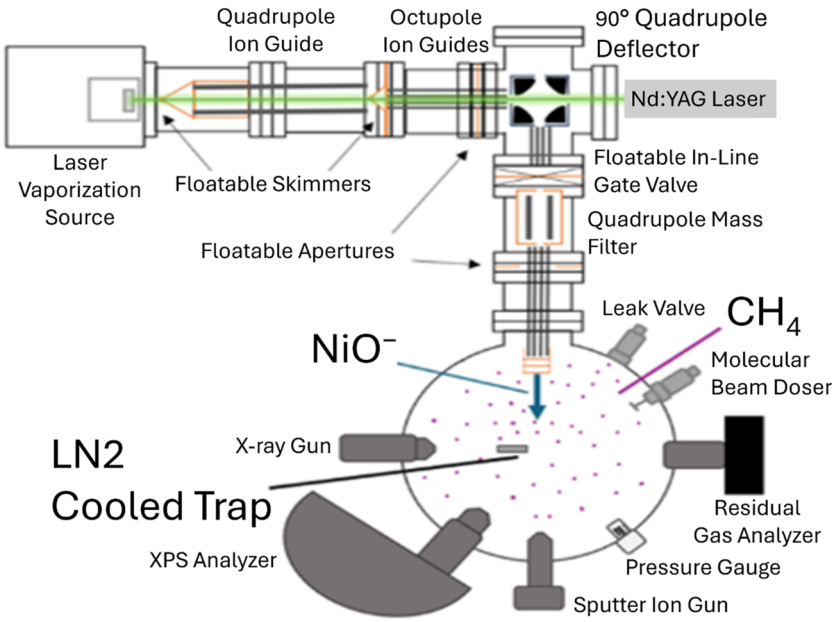

FIG. 3. Schematic of the apparatus used in these experiments.

(10^{-9}–10^{-10} Torr) chamber, where methane was introduced through a variable leak valve in order to raise the pressure in the chamber to 5×10^{-5} Torr. At that pressure, the ion intensity of NiO^- near the middle of the chamber was attenuated by ~10% due to collisions with methane. The collision energy between NiO^- and CH_4 is estimated to have been a few eV due to the low beam energy of ions passing through our quadrupole mass filter. In the same chamber, an annealed highly oriented pyrolytic graphite (HOPG) substrate, which was positioned well away from the NiO^- ion beam trajectory, as illustrated in Fig. 2, to prevent the NiO from depositing onto it, was cooled to below 100 K with liquid nitrogen in order to act as a cryo-trap for collecting the condensable neutral products of the $NiO^- + CH_4$ reaction. After collecting reaction products for ~4 h, the NiO^- ion beam and the methane leak valve were turned off and the methane gas was pumped away. The HOPG substrate with the reaction products frozen on it was then re-positioned via a manipulator to face the entrance of our residual gas analyzer (Hiden model HAL/3F PIC). Upon gradually heating the substrate at a linear heating rate of 1 K/s and monitoring the cationic mass spectra of the desorbed neutral species with the RGA as a function of temperature, i.e., via the TPD technique, the neutral reaction products were identified, either by their parent cations or through their known fragments.

III. RESULTS AND DISCUSSIONS

Figure 4 presents the mass spectrum of the anions formed by pulsing a N_2O/He gas mixture over the laser-ablated Ni rod, recorded by using the quadrupole mass spectrometer in this apparatus. (See Fig. S1 in the supplementary material for a mass spectrum with a higher resolution, recorded by our time-of-flight mass spectrometer apparatus.[15]) Figure 5(a) presents two TPD traces, with the upper panel monitoring CH_3OH^+ (32 amu) and CH_3O^+ (31 amu) ion signals and with the lower panel monitoring CH_2O^+ (30 amu) and CHO^+ (29 amu) ion signals. The sharp, coincident peaks for CH_3OH^+ and CH_3O^+ at 139 K in the upper panel TPD traces of Fig. 5(a) are indicative of methanol formation. According to the NIST database (see Fig. S2 in the supplementary material), the presence of CH_3OH^+ and CH_3O^+ are distinctive signatures for the presence of methanol. Since CH_2O^+ and CHO^+ appear in mass spectral patterns of both methanol and formaldehyde, comparable intensities of CH_2O^+ and CHO^+ in the lower panel TPD traces of Fig. 5(a) suggest that at least some formaldehyde may have also been formed. Interestingly, the lower TPD traces are broader and noisier (lower intensity) than the upper traces, but with their maximum appearing at essentially the same temperature as those of the upper traces. Whether or not some formaldehyde was formed, the data show that methanol was the dominant reaction product. Thus, the present experimental results provided direct support for the previous theoretical calculations.[10,11]

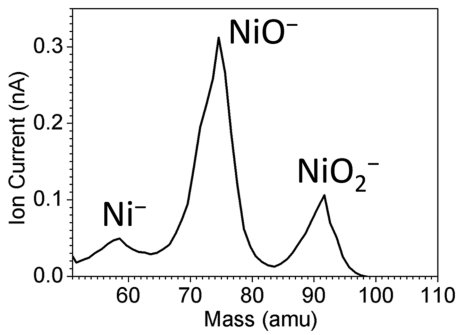

FIG. 4. Anion mass spectrum showing NiO^- generated in these experiments by pulsing a N_2O/He gas mixture over a Ni rod, while it was being laser-ablated by the second harmonic output of a Nd:YAG laser.

Furthermore, in order to confirm that the reaction products were formed in the gas phase by the reaction of $NiO^- + CH_4$ rather than through some unknown and unintended surface reaction with methane, the same experiment was repeated but without NiO^-. A cleaned and annealed HOPG substrate was cooled below 100 K and exposed to methane (5×10^{-5} Torr) for 2 h, resulting in the TPD traces seen in Fig. 5(b). No signals due to methanol or formaldehyde were observed. Furthermore, we performed an additional control experiment, where the NiO molecules were deposited on the HOPG substrate and subsequently exposed to CH_4. As detailed in the supplementary material, no TPD signals of methanol or formaldehyde were observed. These results confirm that the methanol and perhaps formaldehyde observed in Fig. 5(a) were produced by the gas-phase reaction between NiO^- and CH_4. Please note that in these TPD plots (Figs. 5 and S3 in the supplementary material), the trace labeled "CH_3OH^+" represents 32 amu cations. The absence of a desorption peak of the 32 amu cations when the $NiO^- + CH_4$ reaction did not occur also means that the amount of O_2 (32 amu) leaking into the ultra-high-vacuum chamber is negligible in our experimental conditions. Therefore, the mass-selected NiO^- beam is the only source of O atom in a reaction producing CH_3OH.

Quantum chemical calculations specifically focused on the $NiO^- + CH_4$ reaction were performed to further elucidate its mechanism. Molecular structures for all reported intermediate species and transition states were obtained with density functional theory and the MN15 functional.[16] For obtaining more accurate energetics, the gold-standard CCSD(T) level was employed using the MN15 optimized geometries [CCSD(T)//MN15]. For both types of calculations, the aug-cc-pVTZ basis set was employed for all atoms.[17–19] The Gaussian16 software package was invoked for all calculations.[20] All intermediate structures were confirmed to be local minima (only real harmonic vibrational frequencies) and all transition state structures to be first-order saddle points (one imaginary frequency). For all species, the lowest energy state was found to be of doublet spin multiplicity. The reported energies are zero-point vibrational energy corrected electronic energies. The zero-point energy was calculated from the harmonic MN15 vibrational frequencies.

The MN15 structures are depicted in Fig. S4 and the MN15 energy diagram is shown in Fig. S5 in the supplementary material. Compared to the CCSD(T)//MN15 diagram shown in Fig. 6, MN15 predicts more stable intermediate species for the routes forming methanol, while CCSD(T) predicts that the unwanted side products $NiH_2^- + CH_2O$ and $NiCH_2^- + H_2O$ are higher in energy. Table S1 in the supplementary material lists the Cartesian coordinates of all species.

The $NiO^- + CH_4$ reaction mechanisms shown by the quantum chemical calculations are given in the following. Initially, methane transfers a hydrogen atom to either the nickel or oxygen terminus

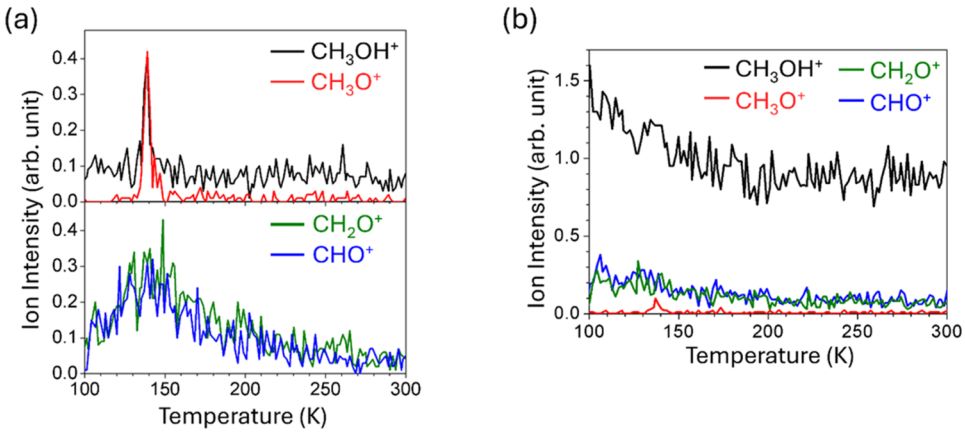

FIG. 5. (a) TPD traces obtained from the HOPG substrate after cold-trapping the products of the NiO^- + CH_4 reaction. The sharp peaks of CH_3OH^+ (32 amu) and CH_3O^+ (31 amu) at 139 K confirm the formation of methanol. The broad features of CH_2O^+ (30 amu) and CHO^+ (29 amu) may imply the formation of some formaldehyde as well. (b) TPD traces obtained from the HOPG substrate while it was kept under 100 K at a methane pressure of 5×10^{-5} Torr for 2 h, during which time the NiO^- beam was off.

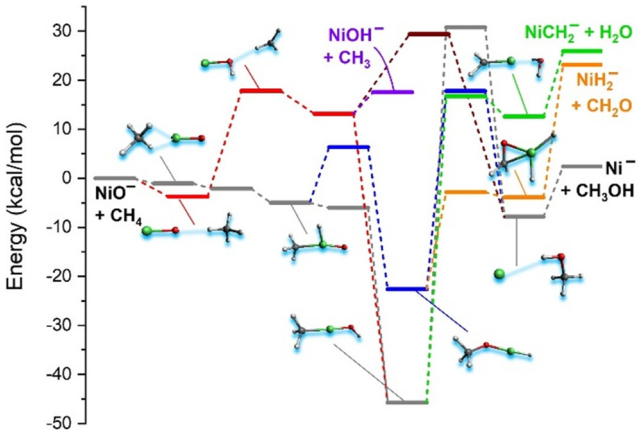

FIG. 6. Energy profile of the various paths for the NiO^- + CH_4 reaction. Structures for the intermediates are also shown (Ni/O/C/H atoms are represented with the green/red/gray/white spheres, respectively); see Figs. S4–S6 in the supplementary material for more information.

of NiO^-, generating either CH_3NiOH^- or $HNiOCH_3^-$. According to our calculations, CH_3NiOH^- is more stable than $HNiOCH_3^-$. These can be formed by two different mechanisms (see Figs. 6 or S4 in the supplementary material for more details). In the first mechanism, methane coordinates to nickel and then transfers its proton to oxygen (gray path of Fig. 6). In the second mechanism, methane approaches oxygen and transfers hydrogen in a remote fashion (red path of Fig. 6). The former path is a low-barrier route, while the latter path has a barrier of about 20 kcal/mol. Release of the unwanted methyl radical ($CH_3^{\cdot}$) from this latter path is unlikely due to the exothermicity and a low activation barrier of the reverse reaction. Both CH_3NiOH^- and $HNiOCH_3^-$ can form methanol by combining the CH_3/OH and H/OCH_3 moieties. The activation barrier for the CH_3/OH recombination step is higher by a factor of 50% compared to H/OCH_3. CH_3NiOH^- may form $NiCH_2^-$ + H_2O byproducts by transferring a hydrogen atom from carbon to oxygen. Similarly, $HNiOCH_3^-$ may form NiH_2^- + CH_2O by transferring a hydrogen atom from carbon to nickel. Both byproducts are unstable (their energies are 20 kcal/mol higher than the desired products, Ni^- + CH_3OH) and are characterized by very low inverse barriers rendering their formation highly unfavorable. Under our experimental conditions, where the collision energy is a few eV, the initial energy of the reactants can support any of the mentioned mechanisms, with the path through CH_3NiOH^- being most probable since it is formed spontaneously. The oxidation step from Ni^- to NiO^- was performed with N_2O, for which theory predicts minimal energy barriers for anions, in contrast with cations.[8]

Overall, the reaction of NiO^- with CH_4 clearly favors the production of CH_3OH over unwanted byproducts, in striking contrast with cationic metal monoxides;[21–23] MnO^+ produces mainly CH_3, FeO^+ forms both CH_3OH and CH_3, PtO^+ forms $PtCH_2^+$, PdO^+ produces CH_3OH and $Pd(CH_2O)^+$, and OsO^+ makes CH_2OsO^+; and only NiO^+ selectively forms CH_3OH. Although the byproducts, $FeCH_2^+$ + H_2O and $Ni(CH_2O)^+$, are more stable than Fe^+/Ni^+ + CH_3OH, they are prevented or suppressed because of correspondingly larger reaction barriers.[24,25] Although the PdO^+ and NiO^+ energy landscapes for their reactions with CH_4 are very similar, only NiO^+ is selective toward CH_3OH, suggesting that its high selectivity may be conditional. On the other hand, the high selectivity for NiO^- is based on thermodynamic arguments and all byproducts are less stable than methanol. Comparing the energy landscapes of NiO^+[22] and NiO^-, this can clearly be attributed to the lower interaction energy between Ni^- and CH_3OH (~10 kcal/mol) vs ~45 kcal/mol between Ni^+ and CH_3OH. This difference results in the energy of the desirable products being lower, making anionic metal monoxides advantageous. For example, if the Ni^-/CH_3OH interaction energy was larger by ~25 kcal/mol, the Ni^- + CH_3OH product would be energetically less favored than the $NiCH_2^-$ + H_2O and NiH_2^- + CH_2O byproducts (see Fig. 6). Indeed, for the NiO^+ + CH_4 cationic reaction, the Ni^+ + CH_3OH product lies at higher energy than the $NiOCH_2^+$ + H_2 product.[10,22]

As a reference, the Ni/CH_3OH interaction energy is at the same level or even lower than that of Ni^-/CH_3OH.[26–28] However, the previous computational studies of the NiO + CH_4 neutral reaction showed that the CH_3 + NiOH formation is kinetically preferred over the Ni + CH_3OH formation.[27,28]

IV. CONCLUSIONS

In conclusion, the partial oxidation of methane to methanol by transition metal monoxide anions was experimentally demonstrated for the first time by allowing NiO^- to react with CH_4 and then characterizing the cold-trapped reaction products via TPD. The quantum chemical calculations showed the reaction mechanisms leading to the selective production of methanol. In particular, the weak interaction between the metal anion and methanol has two beneficial effects: the facile removal of methanol from the metal center and the thermodynamic destabilization of the byproducts. In the solution phase, appropriate solvent molecules and properly designed ligands[11] could be chosen to still further assist in the removal of methanol and to adjust the catalytic performance. The observations reported in this study have the potential to initiate a new direction in molecular catalysis and transform the field of methane activation.[11]

SUPPLEMENTARY MATERIAL

The supplementary material provides the time-of-flight mass spectrum showing NiO^- (Fig. S1); cation mass spectrum patterns of relevant molecules (Fig. S2); supplementary experimental results with NiO molecules deposited on the substrate (Fig. S3); optimized structures for the various pathways of the $NiO^- + CH_4$ reaction at the MN15/aug-cc-pVTZ level of theory (Fig. S4); energy diagram for the various pathways of the $NiO^- + CH_4$ reaction at the MN15/aug-cc-pVTZ level of theory (Fig. S5); energy diagram for the various pathways of the $NiO^- + CH_4$ reaction at the CCSD(T)/aug-cc-pVTZ level of theory (Fig. S6); and Cartesian coordinates for all species in Fig. S5 (Table S1).

ACKNOWLEDGMENTS

The experimental material in this work is based on support from the Air Force Office of Scientific Research (AFOSR) under Grant No. FA9550-22-1-0271 (K.H.B.). The computational material in this work is based on support from the James E. Land endowment and the computational resources were provided by the Auburn University Easley Cluster (E.M.).

AUTHOR DECLARATIONS

Conflict of Interest

The authors have no conflicts to disclose.

Author Contributions

Tatsuya Chiba and Benjamin R. Bilik contributed equally to this work.

Tatsuya Chiba: Investigation (equal); Methodology (equal); Writing – original draft (equal). **Benjamin R. Bilik**: Investigation (equal); Methodology (equal); Writing – original draft (equal). **Kathryn Foreman**: Investigation (equal); Methodology (equal); Writing – original draft (supporting). **Shiying Wang**: Investigation (equal). **Yuheng Han**: Investigation (equal). **Eslam F. M. Abdelazim**: Investigation (equal); Writing – original draft (equal). **Safaa Sader**: Investigation (equal); Writing – original draft (equal). **Evangelos Miliordos**: Conceptualization (equal); Funding acquisition (equal); Investigation (equal); Methodology (equal); Project administration (equal); Resources (equal); Supervision (equal); Validation (equal); Writing – review & editing (equal). **Kit H. Bowen**: Conceptualization (equal); Funding acquisition (equal); Investigation (equal); Methodology (equal); Project administration (equal); Resources (equal); Supervision (equal); Validation (equal); Writing – review & editing (equal).

DATA AVAILABILITY

The data that support the findings of this study are available from the corresponding author upon reasonable request.

REFERENCES

[1] N. F. Dummer, D. J. Willock, Q. He, M. J. Howard, R. J. Lewis, G. Qi, S. H. Taylor, J. Xu, D. Bethell, C. J. Kiely, and G. J. Hutchings, Chem. Rev. **123**, 6359 (2023).
[2] D. C. Upham, V. Agarwal, A. Khechfe, Z. R. Snodgrass, M. J. Gordon, H. Metiu, and E. W. McFarland, Science **358**, 917 (2017).
[3] I. Hussain, S. A. Ganiyu, H. Alasiri, and K. Alhooshani, Coord. Chem. Rev. **497**, 215438 (2023).
[4] G. A. Olah, Angew. Chem., Int. Ed. **44**, 2636 (2005).
[5] M. Ravi, M. Ranocchiari, and J. A. van Bokhoven, Angew. Chem., Int. Ed. **56**, 16464 (2017).
[6] B. G. Hashiguchi, S. M. Bischof, M. M. Konnick, and R. A. Periana, Acc. Chem. Res. **45**, 885 (2012).
[7] A. A. Latimer, A. Kakekhani, A. R. Kulkarni, and J. K. Nørskov, ACS Catal. **8**, 6894 (2018).
[8] E. E. Claveau, S. Sader, B. A. Jackson, S. N. Khan, and E. Miliordos, Phys. Chem. Chem. Phys. **25**, 5313 (2023).
[9] E. E. Claveau, E. R. Heller, J. O. Richardson, and E. Miliordos, J. Phys. Chem. Lett. **14**, 8749 (2023).
[10] S. Sader and E. Miliordos, J. Phys. Chem. A **125**, 2364 (2021).
[11] S. Sader and E. Miliordos, Phys. Chem. Chem. Phys. **24**, 21583 (2022).
[12] J. Jang, K. Shen, and C. G. Morales-Guio, Joule **3**, 2589 (2019).
[13] G.-P. Wei, Y.-X. Zhao, and S.-G. He, J. Chem. Phys. **157**, 154304 (2022).
[14] M. A. Denchy, L. Wang, B. R. Bilik, L. Hansen, S. Albornoz, F. Lizano, N. Blando, Z. Hicks, G. Gantefoer, and K. H. Bowen, J. Phys. Chem. A **126**, 7578 (2022).
[15] T. Chiba, J. A. Olaniyan, S. Wang, Y. Han, E. Miliordos, and K. H. Bowen, J. Phys. Chem. A **129**, 9676 (2025).
[16] H. S. Yu, X. He, S. L. Li, and D. G. Truhlar, Chem. Sci. **7**, 5032 (2016).
[17] N. B. Balabanov and K. A. Peterson, J. Chem. Phys. **123**, 64107 (2005).
[18] T. H. Dunning, Jr., J. Chem. Phys. **90**, 1007 (1989).
[19] R. A. Kendall, T. H. Dunning, Jr., and R. J. Harrison, J. Chem. Phys. **96**, 6796 (1992).
[20] M. J. Frisch, G. W. Trucks, H. B. Schlegel, G. E. Scuseria, M. A. Robb, J. R. Cheeseman, G. Scalmani, V. Barone, G. A. Petersson, H. Nakatsuji, X. Li, M. Caricato, A. V. Marenich, J. Bloino, B. G. Janesko, R. Gomperts, B. Mennucci, H. P. Hratchian, J. V. Ortiz, A. F. Izmaylov, J. L. Sonnenberg, D. Williams-Young, F. Ding, F. Lipparini, F. Egidi, J. Goings, B. Peng, A. Petrone, T. Henderson, D. Ranasinghe, V. G. Zakrzewski, J. Gao, N. Rega, G. Zheng, W. Liang, M. Hada, M. Ehara, K. Toyota, R. Fukuda, J. Hasegawa, M. Ishida, T. Nakajima, Y. Honda, O. Kitao, H. Nakai, T. Vreven, K. Throssell, J. A. Montgomery, Jr., J. E. Peralta, F. Ogliaro, M. J. Bearpark, J. J. Heyd, E. N. Brothers, K. N. Kudin, V. N. Staroverov, T. A. Keith, R. Kobayashi, J. Normand, K. Raghavachari, A. P. Rendell, J. C. Burant, S. S. Iyengar, J. Tomasi, M. Cossi, J. M. Millam, M. Klene, C. Adamo, R. Cammi, J. W. Ochterski, R. L. Martin, K. Morokuma, O. Farkas, J. B. Foresman, and D. J. Fox, *Gaussian 16, Revision C.01*, Gaussian, Inc., Wallingford CT, 2016.
[21] D. Schröder and H. Schwarz, Proc. Natl. Acad. Sci. U. S. A. **105**, 18114 (2008).

[22]A. Božović, S. Feil, G. K. Koyanagi, A. A. Viggiano, X. Zhang, M. Schlangen, H. Schwarz, and D. K. Bohme, Chem. Eur. J. **16**, 11605 (2010).
[23]S. G. Ard, J. J. Melko, V. G. Ushakov, R. Johnson, J. A. Fournier, N. S. Shuman, H. Guo, J. Troe, and A. A. Viggiano, J. Phys. Chem. A **118**, 2029 (2014).
[24]D. C. McDonald II, B. C. Sweeny, S. G. Ard, J. J. Melko, J. E. Ruliffson, M. C. White, A. A. Viggiano, and N. S. Shuman, J. Phys. Chem. A **122**, 6655 (2018).
[25]D. Schroeder, A. Fiedler, J. Hrusak, and H. Schwarz, J. Am. Chem. Soc. **114**, 1215 (1992).
[26]R. Fournier, Theor. Chim. Acta **91**, 129 (1995).
[27]D.-Y. Hwang and A. M. Mebel, J. Phys. Chem. A **106**, 12072 (2002).
[28]H.-Q. Yang, S. Qin, S. Qin, and C.-W. Hu, J. Comput. Chem. **30**, 847 (2009).